ORIGINAL ARTICLE

DNA-Based Prenatal Diagnosis of Harlequin Ichthyosis and Characterization of *ABCA12* Mutation Consequences

Masashi Akiyama[1,5], Matthias Titeux[2,5], Kaori Sakai[1], James R. McMillan[1], Laure Tonasso[2], Patrick Calvas[3], Frederique Jossic[4], Alain Hovnanian[2,3] and Hiroshi Shimizu[1]

Until the identification of *ABCA12* as the causative gene, prenatal diagnosis (PD) for harlequin ichthyosis (HI) had been performed by electron microscopic observation of fetal skin biopsy samples. We report the first case of HI DNA-based PD. Direct sequence analysis of *ABCA12* revealed that the deceased proband was a compound heterozygote for two novel mutations. The maternal nonsense mutation p.Ser1249Term likely leads to nonsense-mediated messenger RNA decay. The paternal mutation c.7436G>A affects the last codon of exon 50 and was expected to be a splice site mutation. For their third pregnancy, the parents requested PD. Direct sequence analysis of fetal genomic DNA from amniotic fluid cells at 17 weeks gestation revealed the fetus was a compound heterozygote for both mutations. The parents requested the pregnancy to be terminated. Analysis of *ABCA12* transcripts of cultured keratinocytes from the abortus showed the presence of six abnormally spliced products from the allele carrying the splice site mutation. Four of them lead to premature termination codons whereas the two others produced shortened proteins missing 21 and 31 amino acids from the second ATP-binding cassette. This report provides evidence for residual ABCA12 expression in HI, and demonstrates the efficiency of early DNA-based PD of HI.

Journal of Investigative Dermatology advance online publication, 2 November 2006; doi:10.1038/sj.jid.5700617

INTRODUCTION

Harlequin ichthyosis (HI) is a severe and usually fatal congenital ichthyosis with an autosomal recessive inheritance pattern (Williams and Elias, 1987; Akiyama, 2006). The clinical features include thick, plate-like scales with ectropion, eclabium, and flattened ears. Infants affected with HI frequently die within the first few weeks of life. Skin development is altered *in utero*; hyperkeratosis of the hair canal occurs in the second trimester and characteristic ultrastructural abnormalities including abnormal lamellar granules, are present in the affected fetal epidermis (Dale *et al.*, 1990; Akiyama *et al.*, 1994, 1998). Before the gene underlying HI was identified in 2005, prenatal diagnosis (PD) of the disease relied on ultrastructural examination of fetal skin biopsy samples at 19–23 weeks estimated gestational age (EGA) (Blanchet-Bardon *et al.*, 1983; Suzumori and Kanzaki, 1991; Akiyama *et al.*, 1994, 1999).

ABCA12 is a transporter which belongs to the ATP-binding cassette (ABC) transporter superfamily (Annilo *et al.*, 2002; Uitto, 2005). In 2005, we identified serious loss of function mutations in *ABCA12* coding an ABC transporter, that leads to defective lipid transport in epidermal keratinocytes and results in an HI phenotype (Akiyama *et al.*, 2005). Another group independently demonstrated that mutations in ABCA12 underlie HI by linkage analysis (Kelsell *et al.*, 2005). Thus, HI PD using molecular *ABCA12* mutational analysis has become possible. We report here the first successful DNA-based PD for HI using fetal genomic DNA specimens from amniotic fluid cells.

RESULTS

Case history and the clinical features of the proband

The newborn proband was the first child from unrelated, healthy French parents. He was affected with HI and died soon after birth. He displayed severe hyperkeratosis with fissures over his entire body, severe ectropion, and eclabium (Figure 1a–c). There was no family history of genodermatoses in the family. The parents had a healthy son, their second child. For their third pregnancy, the parents requested HI PD.

[1]*Department of Dermatology, Hokkaido University Graduate School of Medicine, Sapporo, Japan;* [2]*Inserm, U563 and University Paul Sabatier, Toulouse, France;* [3]*Department of Medical Genetics, Purpan Hospital, Toulouse, France and* [4]*Department of Fetopathology, Nantes Hospital, Nantes, France*

[5]*These authors contributed equally to this work*

Correspondence: Dr Masashi Akiyama, Department of Dermatology, Hokkaido University Graduate School of Medicine, North 15 West 7, Kita-ku, Sapporo 060-8638, Japan. E-mail: akiyama@med.hokudai.ac.jp

Abbreviations: ABC, ATP-binding cassette; cDNA, complementary DNA; EGA, estimated gestational age; HI, harlequin ichthyosis; HIK, HI keratinocytes; LG, lamellar granule; mRNA, messenger RNA; NHK, normal human keratinocytes; PD, prenatal diagnosis

Received 20 June 2006; revised 18 August 2006; accepted 19 September 2006

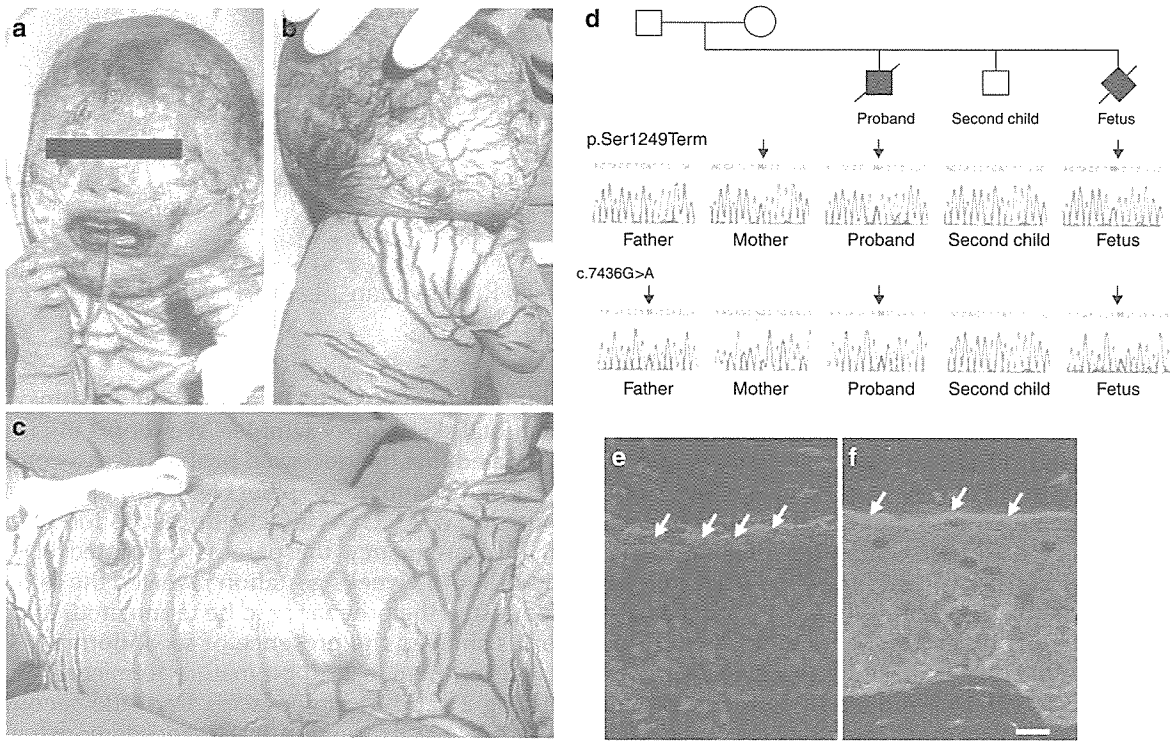

Figure 1. Clinical features of the proband, ABCA12 mutations in the family, and abnormal ABCA12 immunostaining in the patient's epidermis. (**a**, **b**, and **c**) Severe hyperkeratosis with fissures covering (**a**) the proband's face (**b**) scalp and back, (**c**) chest and abdomen. (**a**) Eclabium and (**b**) malformed pinna were apparent. (**d**) A novel nonsense mutation p.Ser1249Term was found in the proband, the mother, and the fetus (arrows). The novel splice site mutation c.7436G>A was detected in the proband, the father and the fetus (arrows). The fetus was prenatally diagnosed as affected. (**e**) In the patient's upper epidermis, weak ABCA12 immunostaining (green: arrows) was seen diffusely in the keratinocyte cytoplasm. (**f**) In normal control human epidermis, intense ABCA12 labeling (green) was noted in the granular layers (arrows). ABCA12, FITC (green); nuclear staining, propidium iodide (red). Bar = 10 μm.

ABCA12 mutation analysis

Mutation analysis of the 53 exons including the intron–exon boundaries of the entire *ABCA12* gene revealed that the proband was a compound heterozygote for two novel *ABCA12* mutations, c.3746C>A and c.7436G>A (sequence according to Lefèvre *et al.* (2003)) (GenBank accession NM 173076) (Figure 1d). c.3746C>A in exon 26 was a novel nonsense mutation that changed a serine residue at codon 1249 to a stop codon (p.Ser1249Term). This nonsense mutation p.Ser1249Term in exon 26 likely leads to nonsense-mediated messenger RNA (mRNA) decay rather than protein truncation, resulting in ABCA12 deficiency (see section *ABCA12* transcript analysis in cultured keratinocytes from the fetus). The mutation p.Ser1249Term was also found in the mother. The other mutation c.7436G>A in exon 50 affects the last amino acid of exon 50 and was expected to be a splice site mutation. Its potential effects on the splicing pattern of *ABCA12* pre-mRNA were investigated (see section *ABCA12* transcript analysis in cultured keratinocytes from the fetus). This splice site mutation was found in the father. Thus, the nonsense mutation p.Ser1249Term was of maternal origin and the splice site mutation c.7436G>A of paternal origin. These mutations were not found in 200 normal alleles (50 French and 50 Japanese healthy unrelated individuals) by sequence analysis, and were unlikely to be polymorphic variations (data not shown).

DNA-based PD of the fetus

Direct sequencing of PCR products including exon 26 or 50 of *ABCA12* from the fetal genomic DNA revealed the presence of the maternal nonsense mutation p.Ser1249Term in exon 26 and the paternal splice site mutation c.7436G>A in exon 50 (Figure 1d). Thus, the fetus harbored both *ABCA12* pathogenic mutations and was predicted to be affected. The pregnancy was terminated at 19 weeks gestation after the parents' request. The fetus showed characteristic changes including thin and fragile skin with petechia, eclabium, small, thickened and abnormally rimmed ears, rigid and swollen fingers and toes.

ABCA12 protein expression in the proband's skin

In the patient, ABCA12 immunostaining in the upper epidermis was reduced (Figure 1e), when compared with the intense ABCA12 immunostaining in the upper epidermal layers, mainly in the granular layers, of normal human skin (Figure 1f).

Ultrastructure of the skin from the abortus

Autopsy skin samples from the abortus showed abnormal, vacuolated lamellar granules in the upper intermediate cells and a large number of lipid droplets in the cytoplasm of incompletely keratinized keratinocytes.

ABCA12 transcript analysis in cultured keratinocytes from the fetus

Analysis of reverse transcription-PCR products from cultured keratinocytes of the fetus HI keratinocyte (HIK) and normal human keratinocytes (NHKs) on agarose gel electrophoresis revealed the presence of a single band in NHK PCR products and three bands in HIK PCR products (data not shown). PCR products were subsequently cloned and sequenced. A total of seven different mRNAs generated from the allele carrying the c.7436G>A mutation were identified (Figure 2a and b). Transcript p.Arg2479Lys corresponds to the full-length *ABCA12* transcript carrying a lysine residue in place of the arginine 2479. In addition, six of these transcripts are generated by splicing from several cryptic splice donor sites located in exon 50 of *ABCA12*. Transcript Δ4 carries a 4 bp deletion around the mutation (c.7433_7436del) leading to a frameshift and a PTC 11 amino acids downstream (p.Arg2479Leufs × 11). Transcript Δ31 displays a 31 bp deletion (c.7406_7436del) leading to a frameshift and a PTC 11 downstream (p.Ile2470_Arg2479 > Leufs × 11). Transcript Δ43 presents a 43 bp deletion (c.7394_7436del) leading to a frameshift and a PTC 11 amino acids downstream (p.Lys2466_Arg2479 > Leufs × 11). Transcript Δ50 shows a 50 bp deletion (c.7387_7436del) leading to a frameshift and a PTC 13 amino acids downstream (p.Asn2464_Arg2479 > Trpfs × 13). Interestingly, transcript Δ63 predicts a truncated protein deleted from Leucine 2459 to Arginine 2479 (p.Leu2459_Arg2479del) owing to an in

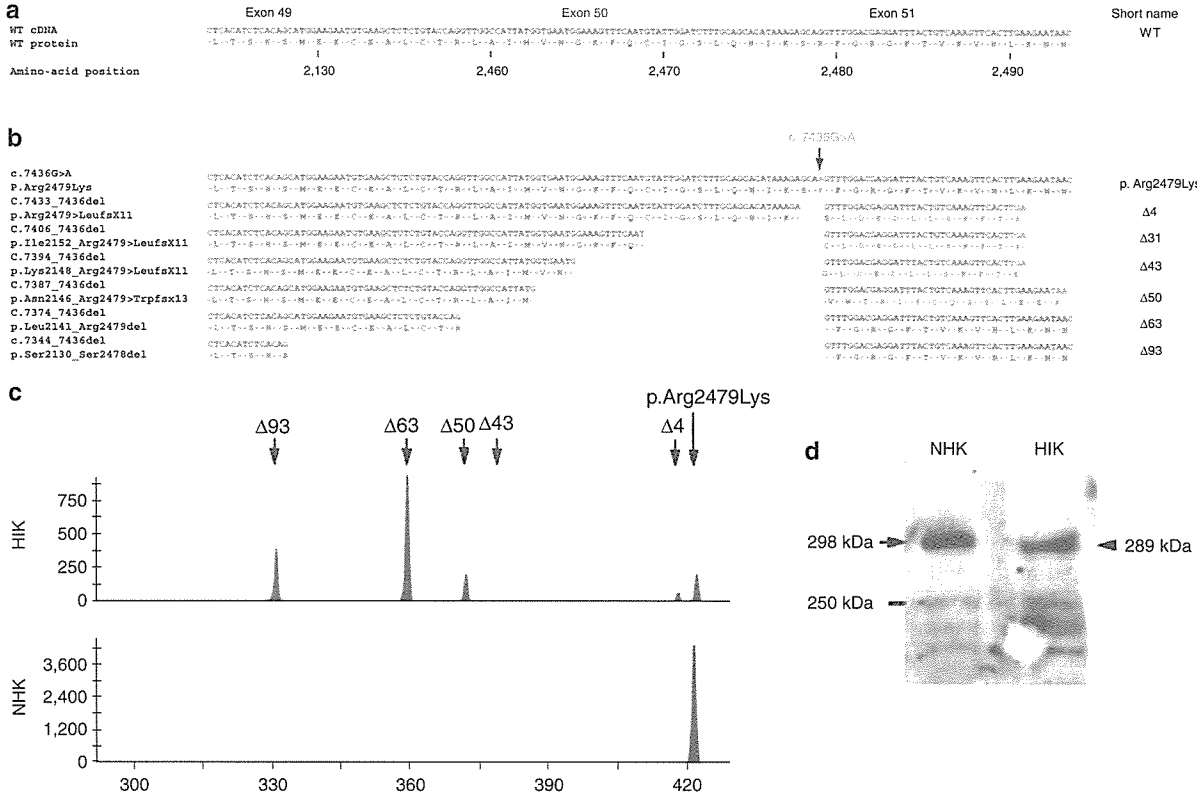

Figure 2. Expression analysis of ABCA12 transcripts and protein. (**a** and **b**) Sequence alignment of the several transcripts generated by the allele carrying the paternal splice site mutation c.7436G>A. (**a**) Wild-type cDNA (blue) and protein sequences of exon 50 of *ABCA12*. Amino-acid numbering is indicated. (**b**) Nucleotide and deduced protein sequences of splice variants of the allele carrying the c.7436G>A mutation (green). Premature stop codons and aberrant sequences owing to frameshifts are indicated in red. Splice variants include the correctly spliced product (p.Arg2479Lys) and six aberrantly spliced forms leading to out-of-frame (transcripts Δ4, Δ31, Δ43, and Δ50) and in-frame (Δ63 and Δ93) deletions. (**c**) Capillary electrophoresis analysis of *ABCA12* cDNA amplimers. Fragments extending over exons 49–53 were amplified by PCR using reverse-transcribed mRNA from primary cultures of HIK and NHKs. Although only one peak at 422 bp is present in NHK, several peaks are detected in HIK. The peak at 422 bp corresponds to the full-length transcript, arising either from the wild-type alleles (in NHK) or from the allele carrying the p.Ser1249Term null mutation and from the allele carrying the p.Arg2479Lys mutation (in HIK). The other peaks at 418, 379, 372, 359, and 329 bp, correspond respectively to transcripts Δ4, Δ43, Δ50, Δ63, and Δ93. The relative amount of each transcript, evaluated by the size of the peaks, shows that transcript Δ63 is predominant. Note that transcript Δ31 is missing, probably because its synthesis level is below the detection threshold of this technique. (**d**) Western blot analysis of ABCA12 protein in NHK and in HIK. A band at 298 kDa (arrow) is present in NHKs extract, however a slightly lower band (arrowhead, 289 kDa) is present in the HIK extracts. This lower band probably arises from the transcript Δ63 and to a less extent from the transcript Δ93.

frame deletion of 63 bp (c.7374_7436del), whereas transcript Δ93 presents an in frame skipping of the entire exon 50 predicting a truncated protein deleted from Serine 2448 to Serine 2478 (p.Ser2448_Ser2478del). The cryptic splice sites used to generate transcripts Δ4, Δ31, Δ50, and Δ63 were predicted using the automated splice site analysis software by Nalla and Rogan (2005).

Capillary electrophoresis analysis of the *ABCA12* complementary DNA (cDNA) amplimers showed one amplimer (422 bp) in NHKs corresponding to the normal sequence of exon 50, whereas five abnormal species were present in HIK (Figure 2c). All but one (Δ31) identified transcripts were found. The relative amount of transcript, indicated by the height of the peaks, showed that the Δ63 transcript is predominant, whereas the Δ31 transcript was not detectable. Interestingly, the height of the peak at 422 bp which arises from both the p.Arg2479Lys transcript and from the transcript synthesized from the other *ABCA12* allele carrying the p.Ser1249Term mutation is weak, indicating that the amount of both transcripts is low. This suggests that the allele carrying the null mutation is likely to be subjected to nonsense mediated mRNA decay and that only a small amount of ABCA12 protein arise from the natural splice site of the pre-mRNA carrying the c.7436G>A.

ABCA12 protein expression in fetal cultured keratinocytes

Western blot analysis revealed the presence of a band of an expected molecular weight of 298 kDa in protein extracts from NHKs, whereas a slightly smaller band of 289 kDa was seen in HI keratinocyte extracts (Figure 2d). This band probably corresponds to the proteins synthesized from both transcript Δ63 and transcript Δ93 which are predicted to encode proteins of calculated molecular weight of 291 and 289 kDa, respectively, and cannot be resolved on the SDS-PAGE. Smaller bands were seen in both extracts and probably correspond to degradation products. Western blot analysis failed to reveal the presence of other shortened proteins in the extract of HIK. However, the epitope recognized by the antibody is located at the end of the C-terminus domain of ABCA12 and thus is not present in the predicted proteins encoded by transcripts Δ4, Δ31, Δ43, and Δ50, and by the product of the allele carrying the p.Ser1249Term mutation.

DISCUSSION

HI is the most severe ichthyotic genodermatosis and has a very poor prognosis. Therefore, any parents' request for PD should be taken very seriously. However, until 2005 the causative gene had not been identified and previous prenatal diagnoses were performed using electron microscopic examination of fetal skin biopsies during the later stages of pregnancies (Blanchet-Bardon *et al.*, 1983; Suzumori and Kanzaki, 1991; Akiyama *et al.*, 1994, 1999). HI PD by fetal skin biopsy was usually performed at 21–22 weeks EGA (Blanchet-Bardon *et al.*, 1983; Suzumori and Kanzaki, 1991; Akiyama *et al.*, 1994, 1999). According to these reports, fetal skin biopsy specimens at that age showed characteristic abnormalities including a large number of lipid droplets in the keratinized cells and abnormal or absent lamellar granules, which were sufficient findings for the PD of the disorder.

However, PD of HI by fetal skin biopsy is technically difficult, requires excellent skin biopsy site selection, and is time-consuming. We need to gain a significant better understanding of fetal skin development and only a few experts are able to make this reliable diagnosis. Owing to the fact that the interfollicular epidermis at 19 weeks EGA or earlier is not sufficiently developed to exhibit the characteristic morphologic changes of keratinization (Holbrook and Odland, 1980), the observations of interfollicular keratinocytes are thought to sometime provide insufficient or unreliable information for PD or prenatal exclusion of HI. However, at 19 weeks EGA, we were able to see characteristic ultrastructural HI abnormalities in the keratinized cells in the hair canal or infundibulum of the developing hair follicle in the case of an affected fetus (Akiyama *et al.*, 1999). This is because keratinization in the hair cone and hair canal occurs at around 15 weeks EGA, approximately 8–9 weeks before the keratinization of interfollicular epidermis in human fetal skin development (Holbrook and Odland, 1978). However, fetal biopsy specimens at 19 weeks EGA may not always provide sufficient information for PD or exclusion of HI because the interfollicular epidermis has not yet keratinized at this stage of epidermal development (Shimizu *et al.*, 2005).

In 2005, *ABCA12* was identified as the underlying gene causing HI (Akiyama *et al.*, 2005; Kelsell *et al.*, 2005). Additional HI cases harboring *ABCA12* mutations have now been reported (Akiyama *et al.*, 2006a, b). Owing to these discoveries, it has now become possible to undertake HI DNA-based PD by chorionic villus or amniotic fluid sampling from the earlier stages of pregnancy. These procedures are technically more reliable and have a reduced burden on the mothers, as in other severe genetic keratinization disorders (Tsuji-Abe *et al.*, 2004). We report here a successful PD of HI using fetal genomic DNA obtained at 17 weeks EGA. It is anticipated that in the future, even earlier prenatal diagnoses using completely non-invasive analysis of DNA from fetal cells in the maternal circulation will be possible (Uitto *et al.*, 2003), as well as pre-implantation genetic diagnosis for HI (Shimizu and Suzumori, 1999).

Expression analysis of *ABCA12* in cultured keratinoctyes from the abortus revealed that the allele carrying the c.7436G>A mutation produced seven different transcripts. The synthesis of six different truncated or deleted transcripts from this allele explains the loss of function of this allele. In particular, transcripts Δ63 and Δ93 predict the synthesis of deleted proteins (deletion of 21 and 31 amino-acid residues, respectively) with calculated molecular weights of 291 and 289 kDa, which cannot be separated on the SDS-PAGE. Thus, the protein detected at 289 kDa is likely to arise from both transcripts, but predominantly from transcript Δ63, which is present in higher amount. The two proteins lack part of the second ATP-binding cassette, which is predicted to dramatically affect ABCA12 function. Although, small amounts of a full-length ABCA12 protein carrying the p.Arg2479Lys mutation may theoretically be synthesized, they were not

detected. Thus, loss of ABCA12 function results from the combination of a null allele, and the synthesis of non-functional deleted proteins unable to restore a normal phenotype.

The terminated fetuses in the previous reports of positive PD of HI showed macroscopic changes consistent with the HI phenotype at 22 weeks or older EGA (Blanchet-Bardon *et al.*, 1983; Suzumori and Kanzaki, 1991; Akiyama *et al.*, 1994, 1999). In our previous report, we demonstrated that an affected fetus already showed a clinically apparent HI phenotype at 21 weeks EGA (Akiyama *et al.*, 1999). Characteristic HI changes of HI were seen both macroscopically and ultrastructurally at 19 weeks EGA and the present case suggests that the HI phenotype has started to emerge in the affected fetus at the late second trimester of pregnancy.

MATERIALS AND METHODS

Mutation detection

Mutational analysis was performed in the proband and both parents. Briefly, genomic DNA isolated from peripheral blood was subjected to PCR amplification, followed by direct automated sequencing using an ABI PRISM 3100 genetic analyzer (ABI Advanced Biotechnologies, Columbia, MD). Oligonucleotide primers and PCR conditions used for amplification of all exons 1–53 of *ABCA12* were originally derived from the report by Lefèvre *et al.* (2003) and were partially modified as described previously (Akiyama *et al.*, 2005). The entire coding region including the exon/intron boundaries for both forward and reverse strands from the proband, the parents and 100 healthy control individuals (50 French and 50 Japanese) were sequenced.

DNA-based prenatal testing

Amniotic fluid cells were obtained under ultrasound guidance at 17 weeks gestation. Fetal DNA was extracted from fresh cells, and detection of *ABCA12* mutations targeting the mutations that were found in the proband was subsequently performed, as described above. There were no sonographic findings suggestive of an affected fetus. No complications arose from the procedure.

Cell culture

Primary human keratinocytes and fibroblasts were obtained from skin fragments of the abortus and a punch biopsy of a healthy control. Keratinocytes were cultured on a feeder layer of lethaly irradiated mouse 3T3-J2 fibroblasts as described previously (Barrandon and Green, 1987). Fibroblasts were grown in DMEM supplemented with 10% heat-inactivated fetal calf serum (Eurobio, Les Ulis, France).

RNA extraction and reverse transcription-PCR analysis

RNA from cultured keratinocytes and fibroblasts was extracted with the SV Total RNA Isolation System (Promega, Charbonnières, France), and first-strand cDNA synthesis was carried out using random hexamer primers and superscript II reverse transcriptase (Invitrogen, Carlsbad, CA). Next, a segment of the *ABCA12* cDNA was PCR-amplified with primers 5′-TCCGTCATCCTCACATCTTCA-3′ (forward) and 5′-GAACCTTGGCTGCTGGTATC-3′ (reverse) using Go-Taq polymerase (Promega, Charbonnières, France). The cDNA amplimers were cloned into PGEM-T vector (Promega, Charbonnières, France) and sequenced using the SP6 primer (5′-ATTTAGGT GACACTATAGAATAC-3′) and the T7 primer (5′-GTAATACGACT CACTATAGGGC-3′). In parallel, the cDNA amplimers were analyzed on standard agarose gel and by capillary electrophoresis on an ABI 310 Genetic Analyzer running the GeneScan software (Applied Biosystems, Foster City, CA).

Immunohistological and immunoblot analysis of ABCA12 protein expression

Immunodetection of ABCA12 was performed using an affinity purified anti-ABCA12 serum raised in rabbits using a 14 amino-acid sequence synthetic peptide (residues 2,567–2,580) derived from the ABCA12 sequence (NM 173076) as the immunogen (Akiyama *et al.*, 2005). Immunofluorescent labeling was performed as described previously (Akiyama *et al.*, 2000). Briefly, 6-μm-thick sections of fresh patient's skin were cut using a cryostat. The sections were incubated in primary antibody solution, anti-ABCA12 antiserum diluted 1/10, for 1 hour at 37°C. The sections were then incubated in FITC-conjugated goat anti-rabbit Igs diluted 1:100 (DAKO, Glostrup, Denmark) for 30 minutes at room temperature, followed by nuclear counterstain by propidium iodide (Sigma Chemical Co., St Louis, MO). The sections were extensively washed with phosphate-buffered saline between incubations. The stained sections were then mounted with a coverslip and observed using a confocal laser scanning microscope. For Western blot analysis, proteins were extracted from cultured keratinocytes in the presence of protease inhibitors (Complete Mini Protease Inhibitor Cocktail, Roche Diagnostics, Meylan, France), fractionated by SDS-PAGE using 30 μg/lane protein on a 4% gel, and transferred to a nitrocellulose membrane (Hybond-C Extra, Amersham Biosciences, Saclay, France). Membrane blocking and incubation with antibody (1:5,000) were carried out in phosphate-buffered saline with 5% skim milk. Secondary antibody was goat anti-rabbit IgG antibodies conjugated to horseradish peroxidase (1:5000, Cell Signalling Technology, Beverley). Signals were revealed with ECL + chemiluminescence reagents (GE Healthcare Bio-Sciences Corp., Piscataway, NJ).

Informed consent was obtained from the patients' parents. This study was approved by the medical ethical committees at the Hokkaido University, Sapporo, Japan, Purpan Hospital, Toulouse, France and Nantes University Hospital, Nantes, France. The study was conducted according to the Declaration of Helsinki Principles.

CONFLICT OF INTEREST

The authors state no conflict of interest.

ACKNOWLEDGMENTS

We thank Ms Megumi Sato, Ms Akari Nagasaki, and Ms Anne-Marie Mazarguil for their technical assistance on this project. This work was supported in part by The GENESKIN European project, the French Ministry of Health (Reference center for orphan skin diseases), Grants-in-Aid from the Ministry of Education, Science, Sports, and Culture of Japan to M. Akiyama (Kiban B. 16390312 and Kiban B. 18390310).

REFERENCES

Akiyama M (2006) Pathomechanisms of harlequin ichthyosis and ABCA transporters in human diseases. *Arch Dermatol* 142:914–8

Akiyama M, Dale BA, Smith LT, Shimizu H, Holbrook KA (1998) Regional difference in expression of characteristic abnormality of harlequin ichthyosis in affected fetuses. *Prenat Diagn* 18:425–36

Akiyama M, Kim D-K, Main DM, Otto CE, Holbrook KA (1994) Characteristic morphologic abnormality of harlequin ichthyosis detected in amniotic fluid cells. *J Invest Dermatol* 102:210–3

Akiyama M, Sakai K, Sugiyama-Nakagiri Y, Yamanaka Y, McMillan JR, Sawamura D *et al.* (2006a) Compound heterozygous mutations including a *de novo* missense mutation in *ABCA12* led to a case of harlequin ichthyosis with moderate clinical severity. *J Invest Dermatol* 126:1518–23

Akiyama M, Sakai K, Wolff G, Hausser I, McMillan JR, Sawamura D *et al.* (2006b) A novel ABCA12 mutation 3270delT causes harlequin ichthyosis. *Br J Dermatol* 155:1064–6

Akiyama M, Smith LT, Shimizu H (2000) Changing patterns of localization of putative stem cells in developing human hair follicles. *J Invest Dermatol* 114:321–7

Akiyama M, Sugiyama-Nakagiri Y, Sakai K, McMillan JR, Goto M, Arita K *et al.* (2005) Mutations in ABCA12 in harlequin ichthyosis and functional rescue by corrective gene transfer. *J Clin Invest* 115:1777–84

Akiyama M, Suzumori K, Shimizu H (1999) Prenatal diagnosis of harlequin ichthyosis by the examinations of keratinized hair canals and amniotic fluid cells at 19 weeks' estimated gestational age. *Prenat Diagn* 19:167–71

Annilo T, Shulenin S, Chen ZQ, Arnould I, Prades C, Lemoine C *et al.* (2002) Identification and characterization of a novel ABCA subfamily member, ABCA12, located in the lamellar ichthyosis region on 2q34. *Cytogenet Genome Res* 98:166–9

Barrandon Y, Green H (1987) Cell migration is essential for sustained growth of keratinocyte colonies: the roles of transforming growth factor-alpha and epidermal growth factor. *Cell* 50:1131–7

Blanchet-Bardon C, Dumez YFL, Lutzner MA, Puissant A, Henrion R, Bernheim A (1983) Prenatal diagnosis of harlequin fetus. *Lancet* 1:132

Dale BA, Holbrook KA, Fleckman P, Kimball JR, Brumbaugh S, Sybert VP (1990) Heterogeneity in harlequin ichthyosis, an inborn error of epidermal keratinization: variable morphology and structural protein expression and a defect in lamellar granules. *J Invest Dermatol* 94:6–18

Holbrook KA, Odland GF (1978) Structure of the human fetal hair canal and initial hair eruption. *J Invest Dermatol* 71:385–90

Holbrook KA, Odland GF (1980) Regional development of the human epidermis in the first trimester embryo and the second trimester fetus (ages related to the timing of amniocentesis and fetal biopsy). *J Invest Dermatol* 74:161–8

Kelsell DP, Norgett EE, Unsworth H, Teh M-T, Cullup T, Mein CA *et al.* (2005) Mutations in ABCA12 underlie the severe congenital skin disease harlequin ichthyosis. *Am J Hum Genet* 76:794–803

Lefèvre C, Audebert S, Jobard F, Bouadjar B, Lakhdar H, Boughdene-Stambouli O *et al.* (2003) Mutations in the transporter ABCA12 are associated with lamellar ichthyosis type 2. *Hum Mol Genet* 12: 2369–78

Nalla VK, Rogan PK (2005) Automated splicing mutation analysis by information theory. *Hum Mutat* 25:334–42

Shimizu A, Akiyama M, Ishiko A, Yoshiike T, Suzumori K, Shimizu H (2005) Prenatal exclusion of harlequin ichthyosis; potential pitfalls in the timing of the fetal skin biopsy. *Br J Dermatol* 153:811–4

Shimizu H, Suzumori K (1999) Prenatal diagnosis as a text for genodermatoses: its past, present and future. *J Dermatol Sci* 19:1–8

Suzumori K, Kanzaki T (1991) Prenatal diagnosis of harlequin ichthyosis by fetal skin biopsy; report of two cases. *Prenat Diagn* 11:451–7

Tsuji-Abe Y, Akiyama M, Nakamura H, Takizawa Y, Sawamura D, Matsunaga K *et al.* (2004) DNA-based prenatal exclusion of bullous congenital ichthyosiform erythroderma at the early stage, 10-11 weeks' of pregnancy in two consequent siblings. *J Am Acad Dermatol* 51:1008–11

Uitto J (2005) The gene family of ABC transporters – novel mutations, new phenotypes. *Trends Mol Med* 11:341–3

Uitto J, Pfendner E, Jackson LG (2003) Probing the fetal genome: progress in non-invasive prenatal diagnosis. *Trends Mol Med* 9:339–43

Williams ML, Elias PM (1987) Genetically transmitted, generalized disorders of cornification; the ichthyoses. *Dermatol Clin* 5:155–78

The South African "Bathing Suit Ichthyosis" Is a Form of Lamellar Ichthyosis Caused by a Homozygous Missense Mutation, p.R315L, in Transglutaminase 1

Journal of Investigative Dermatology advance online publication, 14 September 2006; doi:10.1038/sj.jid.5700550

TO THE EDITOR

Recent years have seen considerable advances in understanding the molecular basis of autosomal-recessive forms of congenital ichthyosis. Indeed, mutations in seven different genes and a further two loci have been implicated. These comprise *TGM1* on 14q11.2 (Huber *et al.*, 1995), *ALOX12B* and *ALOXE-3* on 17p13.1 (Jobard *et al.*, 2002), *ABCA12* on 2q34 (Lefevre *et al.*, 2003), *Ichthyin* on 5q33 (Lefevre *et al.*, 2004), *CGI-58* on 3p21 (Lefevre *et al.*, 2001), *FLJ39501* on 19p12 (Lefevre *et al.*, 2006), and undisclosed genes on 12p11.2–q13 (Mizrachi-Koren *et al.*, 2005) and 19p13.1–p13.2 (Virolainen *et al.*, 2000). Nevertheless, cases of autosomal-recessive congenital ichthyosis display considerable clinical diversity and some phenotypes may be striking and unusual, perhaps indicating further genetic heterogeneity. One such form of autosomal-recessive congenital ichthyosis is "badpak" or bathing suit ichthyosis (BSI), a disorder that is found in parts of South Africa. This condition was first reported in the 1970s (Scott, 1972; Scott and Lups, 1974) and further clinicopathological details have been published recently (Jacyk, 2005). In brief, the characteristic features consist of autosomal-recessive inheritance, skin abnormalities at birth (mainly collodion babies), and large dark grey/brownish scales affecting the trunk and scalp but sparing the central face, buttocks, and limbs. Palms and soles are dry and diffusely mildly hyperkeratotic. The dorsal aspects of the hands and feet appear normal and there are no nail abnormalities. The main feature is the truncal distribution of the ichthyosis which has led to the colloquial term "bathing suit". BSI may not be a uniquely South African genodermatosis, but it has a remarkably consistent phenotype within this population (Scott, 1972; Scott and Lups, 1974; Jacyk, 2005). Skin biopsies have shown orthohyperkeratosis and acanthosis but no discriminating findings (Jacyk, 2005). The aim of this study, therefore, was to determine the molecular basis of this disorder. The fact that BSI only occurs in South Africa and that propagation of an ancestral mutant allele has been suspected led us to perform homozygosity mapping using a single-nucleotide polymorphism (SNP) chip approach.

Following Ethical Committee approval and in compliance with the Declaration of Helsinki Principles, and after obtaining informed consent from all subjects, genomic DNA from eight affected individuals was examined. Those studied were all South African blacks seen in the Department of Dermatology, University of Pretoria, five of which were included in the series recently published by Jacyk (2005). The group consists of three male and five female individuals, aged between 7 and 27 years. The qmain clinical features are illustrated qin Figure 1. Additional details have been described elsewhere (Jacyk, 2005).

To identify the BSI gene, all eight DNA samples were SNP-genotyped using an SNP GeneChip mapping 10K assay according to the manufacturer's instructions (Affymetrix, High Wycombe, UK). Each microarray was scanned using the GeneChip® scanner 3000 and GeneChip® Operating software (GCOS) v1.1.1 with patch 5. The data were analyzed using GeneChip® DNA Analysis Software (GDAS) v3.0. Briefly, 250 ng of genomic DNA was digested with *Xba*I. Adaptor Xba was ligated to the digested DNA and these samples were amplified by PCR with Xba primers. PCR products were fragmented by DNaseI and labeled with biotin. The labeled DNA fragments were then hybridized to the SNP array. Hybridized arrays were processed with an Affymetrix Gene Chip Fluidics Station 450, and fluorescence signals were detected using the Affymetrix GeneChip Scanner 3000. Raw SNP call data were extracted using GeneChip Genotyping Analysis Software and imported into Microsoft Excel for analysis. The average call rate (expressed as a percentage) $\pm$SEM for the eight patients was $80.8 \pm 2.3\%$.

From the SNP assay analysis, seven regions of the genome were found to have large blocks of homozygosity for all affected individuals. Of note, these included a 1.2 Mb interval (22757380–23916597) on chromosome 14q11, which contains the *TGM1* gene. The patients' genomic DNA was therefore amplified with primers specific for *TGM1*, as described elsewhere (Laiho *et al.*, 1997), and the PCR products were sequenced by means of ABI BigDye Terminator reagents (Applied Biosystems, Warrington, UK) in an ABI 310 sequencer.

Sequencing disclosed a homozygous G>T transversion at nucleotide c.944 (GenBank No. NM_000359) in exon 6 of *TGM1* (Figure 2a). This mutation converts an arginine residue to leucine and is designated p.R315L. This mutation was found in all eight DNA samples and is likely to represent

Abbreviations: BSI, bathing suit ichthyosis; SNP, single-nucleotide polymorphism

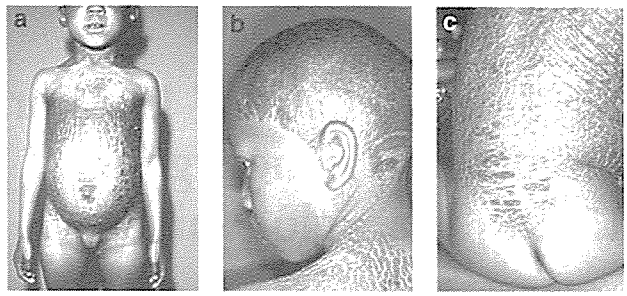

Figure 1. Clinical features of individuals with BSI. Coarse brown/black skin scaling is restricted to (**a**) trunk and (**b**) scalp, sparing the face, (**c**) buttocks, and extremities.

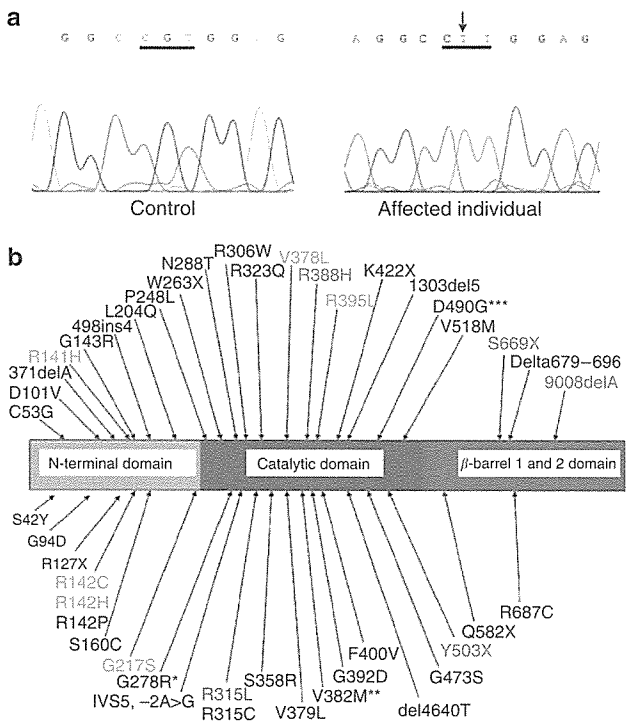

Figure 2. DNA sequencing demonstrates that BSI is due to a homozygous missense mutation in *TGM1* and is therefore allelic to lamellar ichthyosis. (**a**) Sequencing reveals a homozygous single-nucleotide transversion in *TGM1* (NM_000359 c.944G>T) in the affected individuals which converts an arginine residue (CGT) to leucine (CTT), designated p.R315L. (**b**) Illustration of all previously reported mutations in *TGM1* within the postulated sub-domains of the transglutaminase 1 protein (Candi *et al.*, 2005). The resultant clinical phenotypes are indicated by different colors: black, lamellar ichthyosis; blue, non-bullous congenital ichthyosiform erythroderma; green, both lamellar ichthyosis and non-bullous congenital ichthyosiform erythroderma; red, the mutation defined in BSI, although a case of classical lamellar ichthyosis with this mutation has also been reported (ref. Tok *et al.*, 1999). *Self-healing collodion baby as well as lamellar ichthyosis has been reported for this mutation (Raghunath *et al.*, 2003). **A case of lamellar ichthyosis sparing the face and extremities, with some clinical similarities to BSI, has been reported for this mutation (Petit *et al.*, 1997). ***Self-healing collodion baby with no residual scaling has been reported for this mutation (Raghunath *et al.*, 2003). One further unrepresented mutation in the promoter region (−86C>T) has been reported in a case of lamellar ichthyosis (Cserhalmi-Friedman *et al.*, 2001).

a founder effect in this population. Indeed, several of the affected individuals belong to the Nguni ethnic groups (Zulu, Swazi, and Xhosa). No other sequence variations were identified in the coding or splice site regions. The p.R315L substitution was not identified as a polymorphism by screening 50 ethnically matched control genomic DNA samples.

This molecular analysis indicates that BSI is a particular form of lamellar ichthyosis caused by a homozygous missense mutation, p.R315L, in the *TGM1* gene which encodes transglutaminase 1. This enzyme has a vital role in the formation of the cornified cell envelope by crosslinking several precursor proteins (such as involucrin) and in crosslinking hydroxyceramide to the cornified cell envelope (Candi *et al.*, 2005). Loss or reduction of its activity leads to defective cornified cell envelope formation and collapse of the stratum corneum lipid barrier. More than 40 different *TGM1* mutations have now been identified (see Figure 2b). These have been associated with various autosomal-recessive forms of congenital ichthyosis phenotypes usually called lamellar ichthyosis or non-bullous congenital ichthyosiform erythroderma. In some reports, however, other forms of ichthyosis have also been ascribed to *TGM1* mutations (Raghunath *et al.*, 2003).

The mutated arginine we identified in the BSI individuals is likely to be pathogenic as it is located within the core domain of transglutaminase 1, a site involved in stabilizing the structural conformation of the enzyme through salt bridge and hydrogen bonds linked to neighboring amino acids (Huber *et al.*, 1997). Furthermore, arginine 315 is highly conserved throughout the transglutaminase family. Remarkably, the p.R315L mutation in *TGM1* has been previously reported in African-American twins with a more classical phenotype of lamellar ichthyosis (Tok *et al.*, 1999). In those cases, skin scaling was very extensive, sparing only the face and the flexures, and did not show a "bathing suit" distribution.

How can the unusual and striking, patchy but consistent, skin involvement in BSI be explained? The pattern of involvement is not in keeping with any particular segmental distribution or form of mosaicism – it is clearly a fully penetrant autosomal-recessive disorder with minimal inter- and intra-familial variability. It appears to be a distinct clinical disorder, although one case of

lamellar ichthyosis sparing the face and the four limbs, with some similarities to BSI, has been reported (Petit *et al.*, 1997). Indeed, the presence of involved and uninvolved skin with varying clinical presentations in several other cases of autosomal-recessive congenital ichthyosis is well recognized but poorly understood because of limited insight from genotype–phenotype correlation studies (Akiyama, 2006). A comparative study of involved and uninvolved skin in lamellar ichthyosis resulting from *TGM1* mutations showed reduced TGM1 activity in both affected and unaffected skin but more so in the affected regions (Petit *et al.*, 1997). The sparing of the extremities and face in BSI suggests that the p.R315L mutation may not abolish the activity of transglutaminase 1 completely, but this does not explain the peculiar scaling pattern seen in all cases of BSI.

In summary, we have determined that the South African bathing suit form of ichthyosis is a variant of lamellar ichthyosis associated with *TGM1* gene pathology. Delineation of a specific mutation in the form of p.R315L has important implications for the affected population in South Africa. We estimate that there are at least 50 affected families within the Pretoria and Johannesburg districts, and therefore knowledge of the molecular basis of BSI will be very helpful in improving genetic counseling within this South African population.

CONFLICT OF INTEREST

The authors state no conflict of interest.

Ken Arita[1,2], Witold K. Jacyk[3], Vesarat Wessagowit[1,4], Elizabeth Jansen van Rensburg[5], Tracy Chaplin[6], Charles A. Mein[7], Masashi Akiyama[2], Hiroshi Shimizu[2], Rudolf Happle[8], John A. McGrath[1]

[1]Genetic Skin Disease Group, St John's Institute of Dermatology, Division of Genetics and Molecular Medicine, The Guy's, King's College and St Thomas' School of Medicine, St Thomas' Hospital, London, UK; [2]Department of Dermatology, Hokkaido University Graduate School of Medicine, Sapporo, Japan; [3]Department of Dermatology, University of Pretoria, Pretoria, South Africa; [4]Institute of Dermatology, Bangkok, Thailand; [5]Department of Genetics, University of Pretoria, Pretoria, South Africa; [6]CRUK Medical Oncology, London, UK; [7]Barts and the London, Queen Mary's School of Medicine and Dentistry, London, UK and [8]Department of Dermatology, University of Marburg, Marburg, Germany.
E-mail: ken_arita222@yahoo.co.jp

REFERENCES

Akiyama M (2006) Harlequin ichthyosis and other autosomal recessive congenital ichthyoses: the underlying genetic defects and pathomechanisms. *J Dermatol Sci* 42:83–9

Candi E, Schmidt R, Melino G (2005) The cornified envelope: a model of cell death in the skin. *Nat Rev Mol Cell Biol* 6:328–40

Cserhalmi-Friedman PB, Milstone LM, Christiano AM (2001) Diagnosis of autosomal recessive lamellar ichthyosis with mutations in the TGM1 gene. *Br J Dermatol* 144:726–30

Huber M, Rettler I, Bernasconi K, Frenk E, Lavrijsen SP, Ponec M *et al.* (1995) Mutations of keratinocyte transglutaminase in lamellar ichthyosis. *Science* 267:525–8

Huber M, Yee VC, Burri N, Vikerfors E, Lavrijsen AP, Paller AS *et al.* (1997) Consequences of seven novel mutations on the expression and structure of keratinocyte transglutaminase. *J Biol Chem* 272:21018–26

Jacyk WK (2005) Bathing-suit ichthyosis: a peculiar phenotype of lamellar ichthyosis in South African blacks. *Eur J Dermatol* 15:433–6

Jobard F, Lefevre C, Karaduman A, Blanchet-Bardon C, Emre S, Weissenbach J *et al.* (2002) Lipoxygenase-3 (*ALOXE3*) and 12(*R*)-lipoxygenase (*ALOX12B*) are mutated in non-bullous congenital ichthyosiform erythroderma (NCIE) linked to chromosome 17p13.1. *Hum Mol Genet* 11:107–13

Laiho E, Ignatius J, Mikkola H, Yee VC, Teller DC, Niemi KM *et al.* (1997) Transglutaminase 1 mutations in autosomal recessive congenital ichthyosis: private and recurrent mutations in an isolated population. *Am J Hum Genet* 61:529–38

Lefevre C, Audebert S, Jobard F, Bouadjar B, Lakhdar H, Doughdene-Stambouli U *et al.* (2003) Mutations in the transporter ABCA12 are associated with lamellar ichthyosis type 2. *Hum Mol Genet* 12:2369–78

Lefevre C, Bouadjar B, Ferrand V, Tadini G, Megarbane A, Lathrop M *et al.* (2006) Mutations in a new cytochrome *P*450 gene in lamellar ichthyosis type 3. *Hum Mol Genet* 15:767–76

Lefevre C, Bouadjar B, Karaduman A, Jobard F, Saker S, Ozgue M *et al.* (2004) Mutations in *ichthyin* a new gene on chromosome 5q33 in a new form of autosomal recessive congenital ichthyosis. *Hum Mol Genet* 13:2473–82

Lefevre C, Jobard F, Caux F, Bouadjar B, Karaduman A, Heilig R *et al.* (2001) Mutations in *CGI-58*, the gene encoding a new protein of the esterase/lipase/thioesterase subfamily, in Chanarin–Dorfman syndrome. *Am J Hum Genet* 69:1002–12

Mizrachi-Koren M, Geiger D, Indelman M, Bitterman-Deutsch O, Bergman R, Sprecher E (2005) Identification of a novel locus associated with congenital recessive ichthyosis on 12p11.2–q13. *J Invest Dermatol* 125: 456–62

Petit E, Huber M, Rochat A, Bodemer C, Teillac-Hamel D, Muh JP *et al.* (1997) Three novel point mutations in the keratinocyte transglutaminase (TGK) gene in lamellar ichthyosis: significance for mutant transcript level, TGK immunodetection and activity. *Eur J Hum Genet* 5:218–28

Raghunath M, Hennies HC, Ahvazi B, Vogel M, Reis A, Steinhert PM *et al.* (2003) Self-healing collodion baby: a dynamic phenotype explained by a particular transglutaminase-1 mutation. *J Invest Dermatol* 120:224–8

Scott F (1972) Skin diseases in the South African Bantu. In: *Essays on Tropical Dermatology.* (Marshall J, ed), vol. 2. Amsterdam: Excerpta Medica, 1–17

Scott FP, Lups JHG (1974) Badpak-distrubusie van lamellêre igtiose in de Bantoe: 'n nuwe entiteit. *South Afr Med J* 48:2449–53

Tok J, Garzon MC, Cserhalmi-Friedman P, Lam HM, Spitz JL, Christiàno AM (1999) Identification of mutations in the transglutaminase 1 gene in lamellar ichthyosis. *Exp Dermatol* 8: 128–33

Virolainen E, Wessman M, Hovatta I, Niemi KM, Ignatius J, Kere J *et al.* (2000) Assignment of a novel locus for autosomal recessive congenital ichthyosis to chromosome 19p13.1–p13.2. *Am J Hum Genet* 66:1132–7

doi: 10.1111/j.1365-2230.2006.02262.x

Giant dermatofibroma: a rare variant of dermatofibroma preferentially developing on the lower limbs

D. Hoshina, A. Shibaki, S. Aoyagi, K. Kimura and H. Shimizu

Department of Dermatology, Hokkaido University Graduate School of Medicine, N15 W7, Kita-ku, Sapporo 060–8638, Japan

A 20-year-old man presented to our outpatient clinic with a 3-year history of a slowly growing nodule on his right leg. Physical examination revealed a brown, firm nodule, 50 mm in diameter, which was immobile owing to the adhesion to the subcutaneous tissue (Fig. 1a). The surface of the nodule was moderately hyperkeratotic and partly covered with brown crusts. An initial incisional biopsy demonstrated an irregularly arranged dense proliferation of fibroblast-like cells throughout the dermis and superficial subcutaneous tissue. Magnetic resonance imaging demonstrated invasion close to the fascia of the anterior tibial muscle (Fig. 1b). A simple surgical excision was made for diagnosis and treatment.

Histopathological examination revealed a relatively sparse proliferation of fibroblast-like tumour cells without nuclear atypia throughout the entire dermis (Fig. 2a). The overlying epidermis demonstrated moderate hyperkeratosis (Fig. 2b). The tumour cells were loosely arranged within the mature collagen bundles (Fig. 2c) and partially extended into the superficial subcutaneous tissue along the fibrous septa (Fig. 2d). Immunohistochemical examination demonstrated a lack of CD34 expression in the proliferating tumour cells. From the histopathological and immunohistochemical features, a diagnosis of giant dermatofibroma (DF) was made.

DF is a benign cutaneous tumour, generally <20 mm in diameter.[1] However, these tumours sometimes enlarge and may be misdiagnosed as malignant tumours, such as dermatofibrosarcoma protuberans (DFSP). Giant DF is a clinical variant of DF, designated by Danckaert and Karassik in 1975[1] and characterized by its unusually large size. Although there is no clear definition of the size for the diagnosis of giant DF, Requena *et al.*[2] used a size larger than 35 mm for the diagnosis of giant DF in their study. In previous reports, the size of the tumour ranged from 35 to 120 mm, and almost all the lesions were located on the lower limbs.[1–3] No recurrence after surgical excision has been reported to date.[2]

Distinguishing giant DF from malignant fibrous tumours, especially DFSP, may be difficult, owing to its unusual clinical appearance. Although histopathological examination reveals conventional features of DF in most cases, an incisional biopsy specimen from the tumour may demonstrate architectural features similar to DFSP. In order to distinguish between the two entities of giant DF and DFSP, several reports have suggested that immunohistochemical analysis of CD34 and factor XIIIa expression is useful.[4] However, even these methods could fail to lead to a diagnosis because there may be staining variability among different cases. Focal CD34 reactivity may be demonstrated in some DF cases,[4,5] whereas some DFSPs uncharacteristically express factor XIIIa, but not CD34.[4,5] Recently, Cribier *et al.* reported that immunohistochemical staining of stromelysin 3 (ST3) may be useful for the distinction in such problematic cases. In their study, none of the 40 DFSP cases expressed ST3, while all 40 DF cases, including 10 giant DFs, expressed ST3.[5]

In our case, initial incisional biopsy was insufficient to permit a definite diagnosis to be made. Careful histopathological re-evaluation of the surgical specimens revealed that most of the tumour showed the typical histopathological features of DF. In addition, the negative result of immunohistochemical staining with anti-CD34 supported the diagnosis of giant DF.

We suggest that a thorough histopathological examination of large tissue samples from the tumour, together with immunohistochemical staining, is recommended for the correct diagnosis of giant DF.

Correspondence: Dr Akihiko Shibaki, MD, PhD, Department of Dermatology, Hokkaido University Graduate School of Medicine, North 15 West 7, Kita-ku, Sapporo 060-8638, Japan.
E-mail: ashibaki@med.hokudai.ac.jp

Conflict of interest: none declared.

Accepted for publication 30 June 2006

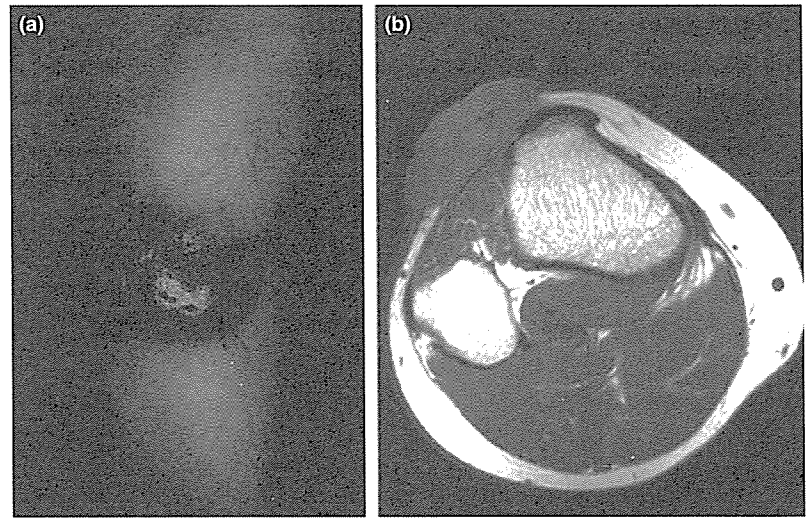

Figure 1 (a) Brown, firm nodule, 50 mm in diameter, immobile owing to adhesion to the subcutaneous tissue; (b) magnetic resonance imaging demonstrated invasion close to the fascia of the anterior tibial muscle.

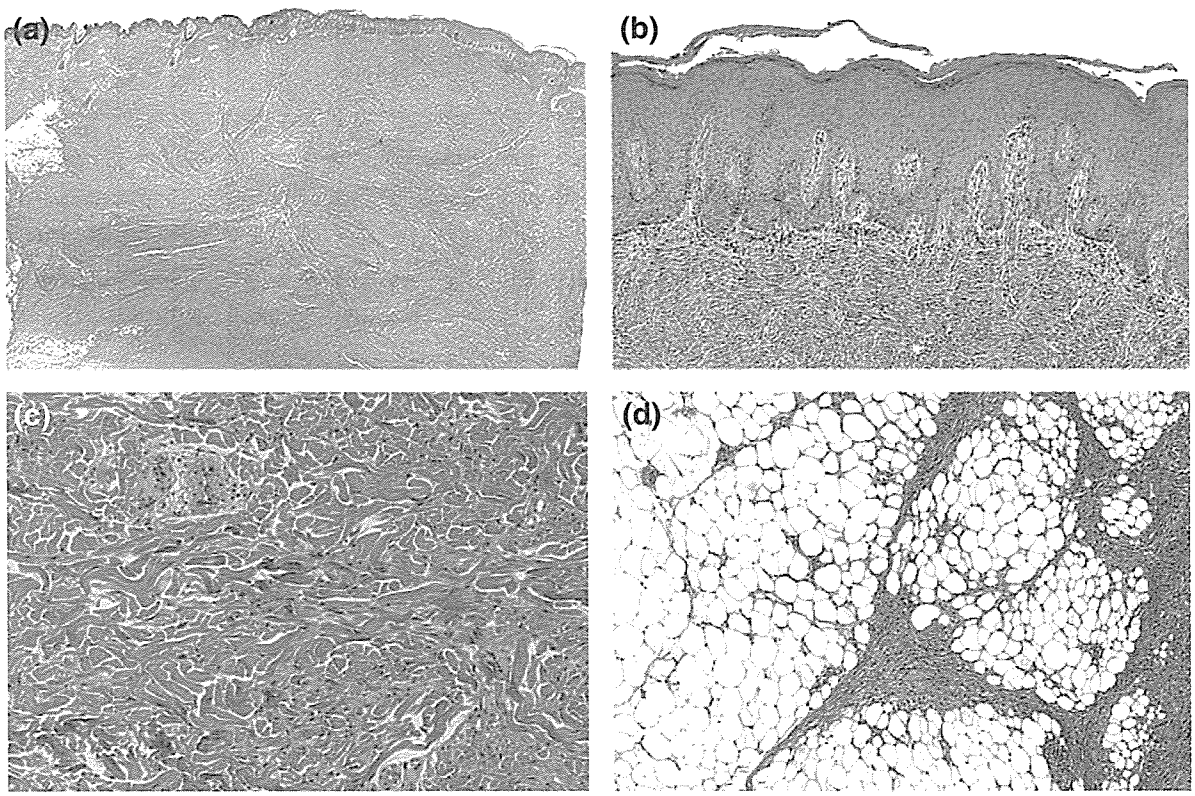

Figure 2 (a) A relatively sparse proliferation of fibroblasts without nuclear atypia, which produced mature collagen bundles throughout the entire tumour. (b) the overlying epidermis demonstrated moderate hyperplasia; (c) most of the tumour was occupied by an area with a sparse number of cells, comprised of plump spindle cells producing mature collagen bundles; (d) the subcutaneous invasion preserved the fat lobules. Haematoxylin and eosin, original magnification (a) ×5, (b–d) ×100.

References

1 Danckaert B, Karassik SL. Dermatofibroma: An usual presentation. *Cutis* 1975; **16**: 245–7.
2 Requena L, Farina MC, Fuente C *et al.* Giant dermatofibroma. A little known clinical variant of dermatofibroma. *J Am Acad Dermatol* 1994; **30**: 714–19.
3 Goolman HB, Sanders LJ, Porter MC. Benign fibrous histiocytoma of the foot: a literature review and case report. *Cutis* 1990; **46**: 223–6.
4 Goldblum JR, Tuthill RJ. CD34 and factor-XIIIa immunoreactivity in dermatofibrosarcoma protuberans and dermatofibroma. *Am J Dermatopathol* 1977; **19**: 147–53.
5 Cribier B, Noacco G, Peltre B, Grosshans E. Stromelysin 3 expression: a useful marker for the differential diagnosis dermatofibroma versus dermatofibrosarcoma protuberans. *J Am Acad Dermatol* 2002; **46**: 408–13.

Technical Report to Nature Medicine

Humanization of autoantigen

Wataru Nishie[1*], Daisuke Sawamura[1*], Maki Goto[1], Kei Ito[1], Akihiko Shibaki[1], James R. McMillan[1], Kaori Sakai[1], Hideki Nakamura[1], Edit Olasz[2], Kim B. Yancey[2], Masashi Akiyama[1], Hiroshi Shimizu[1].

[1] Department of Dermatology, Hokkaido University Graduate School of Medicine, Sapporo, Japan.

[2] Department of Dermatology, Medical College of Wisconsin, Milwaukee, Wisconsin, USA.

[*] These 2 authors contributed equally as first authors to this work

Address for correspondence:
Hiroshi Shimizu, M.D., Ph.D.,
Department of Dermatology, Hokkaido University Graduate School of Medicine,
N15 W7, Sapporo, 060-8638, Japan.
Phone: +81-11-761-1161
Fax: +81-11-706-7820
E-mail: shimizu@med.hokudai.ac.jp

Transmissibility of characteristic lesions to experimental animal provides potential for understanding the pathomechanism of human autoimmune disease. Here we demonstrate, the ability to reproduce human autoimmune disease using genetically-engineered model mice. Bullous pemphigoid (BP) is the most common serious autoimmune blistering skin disease, with a considerable body of indirect evidence indicating that the underlying autoantigen is collagen XVII (COL17). Passive transfer of human BP autoantibodies into mice has failed to induce skin lesions, probably due to differences in amino acid sequence of the COL17 pathogenic epitope between humans and mice. In this study, human BP autoantibody was injected into murine COL17 knockout mice rescued by the human ortholog. This led to the successful generation of the BP-like skin lesions and a human disease phenotype. Humanization of autoantigens can be a newly developed approach of research in human autoimmune diseases.

Evolution of a complex immune system in mammals can paradoxically lead to an increased likelihood of autoimmune disease, which affects ~5 % of the general population [1]. The immune system comprises two evolutionally different responses, innate immunity and adaptive immunity. Vertebrates are capable of both adaptive and innate immunity that is common to all metazoans, and are consequently exposed to possible autoimmune diseases, whereby an aberrant, adaptive immune system recognizes a self component as an autoantigen. To understand the pathogenesis of these diseases and to develop novel therapies, animal models corresponding to human autoimmune diseases are essential [2, 3]. A small number of experimental animal models of autoimmune diseases have been generated by passive transfer of autoantibodies from patients [4, 5], but this approach has not been universally successful due to limited interspecies recognition of the autoantigen by the adaptive immune system. In reality, most animal models that reflect human autoimmune diseases have been identified from spontaneously arising diseases or have been generated by repeated immunization using host candidate autoantigens [2, 3]. While these animal models may develop certain aspects of human autoimmune diseases, there is as yet no reliable method to produce models that identically and faithfully reproduce human autoimmune disorders. Recently, transgenic mice expressing disease-associated human HLA alleles and T-cell receptors have been generated, which have the potential to provide further insight into the pathogenesis of many diseases [2, 3, 6, 7]. Conversely, few advances have been made to humanize autoantigens in animals. Our study has therefore focused on this approach in the disease BP, the most common antibody-mediated autoimmune blistering skin disease. Although the sera of BP patients are known to contain autoantibodies against the collagen XVII (COL17) autoantigen, direct proof of the pathogenicity of COL17 autoantibodies has not been unequivocally proven due to failure of previous passive transfer experiments [8, 9]. In the native COL17 epidermal protein,

the pathogenic epitope is restricted to the non-collagenous 16 A (NC16A) domain [10] that shows distinct diversity among different species [8, 9]. In this study, to assess the direct pathogenicity of human BP autoantibodies in a mouse model, we have humanized the murine BP autoantigen. Furthermore, we have used this novel mouse to show that COL17 decoy peptides block the pathogenic activity of BP IgG *in vivo*.

RESULTS

Generation of COL17-humanized (*COL17* $^{m-/-, h+}$) mice

We first generated COL17 knockout (*COL17* $^{m-/-}$) mice, in which the phenotypic features closely resembled the human disease non-Herlitz epidermolysis bullosa (OMIM: 226650) caused by null mutations in the *COL17A1* gene (Fig. 1) [11-13]. When *COL17* $^{m-/-}$ mice were born, blisters and erosions at sites of trauma were easily created after mild friction, and some pups displayed spontaneous blister formation on their paws (Fig. 1 f). Other characteristic findings seen in adult *COL17* $^{m-/-}$ mice were genital erosions, hemorrhagic blisters around the digits, and diffuse, non-pigmented hair growth associated with hair loss (Fig. 1 g, h). *COL17* $^{m-/-}$ mice showed growth retardation compared with wild type littermates; most *COL17* $^{m-/-}$ mice died within 2 weeks of birth. Mortality rates of the *COL17* $^{m-/-}$ and wild type littermates at 8 weeks were 80.1 % and 4.0%, respectively (Supplementary Fig. 1).

Next, we rescued *COL17* $^{m-/-}$ mice by mating them with C57BL/6Ncr mice expressing human COL17 under the control of a human keratin 14 promoter (*COL17* $^{h+}$) (Olasz et al, manuscript submitted). After crossing heterozygote *COL17* $^{m-/+}$ mice and human COL17 transgenic (*COL17* $^{m+/+, h+}$) mice, rescued COL17-humanized (*COL17* $^{m-/-, h+}$) mice were generated. Interestingly, rescued COL17-humanized mice showed none of the abnormal manifestations seen in *COL17* $^{m-/-}$ mice (Fig. 2 a, and Supplementary Fig. 1b). Remarkably, the rescued mice exhibited reproductive ability despite the fact that the original *COL17* $^{m-/-}$ mice were unable to multiply.

Passive transfer of pathogenic IgG from BP patients into COL17-humanized mice

We then performed a passive transfer study using pathogenic IgG from BP patients. Preliminary studies in human COL17 transgenic (*COL17* $^{m+/+, h+}$) mice failed to demonstrate skin detachment (data not shown), therefore we studied neonatal COL17-humanized mice instead. The COL17-humanized mice, which received intra-peritoneal injections of both total as well as affinity purified IgG directed against COL17 developed diffuse erythema and a positive Nikolsky sign (epidermal separation/blistering elicited by gentle skin friction) at 48 h after injection (Fig. 2 e, and Table 1). Histopathologic studies of lesional skin revealed a separation between the epidermis and dermis, and an inflammatory cell infiltrate including neutrophils and lymphocytes (Fig. 2 e). Direct immunofluorescence studies

revealed a linear deposition of human IgG along the dermal-epidermal junction (Fig. 2 f). Electron microscopic findings revealed dermal-epidermal separation in the lamina lucida between the plasma membrane of basal keratinocytes and the lamina densa (Fig. 2 g). All these findings are consistent with, and precisely recapitulate, human BP skin lesions[14], thus confirming that these animals are excellent models for human BP disease initiated by an interaction between human BP autoantibodies and the human COL17 adhesion protein.

Epitope decoy therapy using recombinant COL17 antigenic peptides in BP model mice

Finally, using this animal system, we have evaluated the efficiency of a novel approach to therapy for BP. We synthesized 6 different short peptides overlapping a variety of antigenic COL17 NC16A microdomains (Fig. 3 a). *In vitro* immune-adsorption studies demonstrated that a 77 amino acid recombinant peptide (R1) most efficiently suppressed the BP antibody index value (all index value against BP antibody was referred to the COL17 NC16A domain peptide, see Methods section) from BP patient sera (Fig. 3 b and Supplementary Method). Furthermore, we found that the suppression efficacy of R1 was increased after fusion with glutathione-S-transferase (GST) to R1 (Fig. 3 b). This R1-GST peptide reduced index values of BP IgG in a dose-dependant manner in an *in vitro* binding assay (Fig. 3 c). After intra-peritoneal injection with 1 mg/g body weight total IgG from BP patients, COL17-humanized mice were treated with R1-GST peptide (total dose of 600μg, injected subcutaneously), resulting in marked reduction in blister formation (specifically, no blisters or skin fragility in 16 of 17 mice), in contrast to controls treated with GST alone (extensive blisters in 12 of 16 mice) (Fig. 3 d, e). Histopathologically, R1-GST treated mouse skin showed no subepidermal blister formation, while distinctive blister formation developed in control mouse skin (Fig. 3 d). Direct immunofluorescence studies revealed a significantly reduced amount of IgG immune-deposition at the BMZ in the recombinant protein treated group compared with that of control group (Fig. 3 d). BP antibody index value also showed significantly decreased in the treated group (Fig. 3 f, $n=15$, $p<0.01$). No adverse reactions to the peptide treatments, including features of anaphylaxis or dermatitis, were observed.

DISCUSSION

This study is the first to succeed in generating a *COL17* $^{m-/-}$ mouse. Moreover, the generation of COL17-humanized (*COL17* $^{m-/-, h+}$) mice with a normal appearance clearly demonstrates that the transgenic epidermal COL17 product that originated from the transfected COL17 cDNA is able to abolish the clinical features of the *COL17* $^{m-/-}$ mouse. This supports the previously proposed notion that genetic diseases with defective epidermally expressed genes, such as those in the epidermolysis bullosa group of diseases, can be treated by gene therapy using an appropriate cDNA, even from another species.

The potential pathogenic role of COL17 has been supported in an experimental murine passive transfer model utilizing rabbit IgG directed against the murine homolog of the immunodominant epitope of human COL17 [9]. Indeed, many previous attempts have been made to try to confirm the pathogenicity of human COL17 BP autoantibodies directly. Of note, Zillikens *et al.* developed a further model by administering IgG fractions from BP patients into human skin grafted onto adult severe combined immunodeficient (SCID) mice. However, no blister formation was observed, although human IgG and murine C3 were both deposited at the epidermal basement membrane zone of the grafted human skin [15].

Here, we have been the first to be able to generate BP lesions in experimental animals using human BP patient autoantibodies. Several factors have contributed to the success of this model system. First, rescued COL17-humanized mice possess a functional, humanized COL17 protein that is faithfully recognized by IgG autoantibodies from our human BP patients. Second, we performed this passive transfer study using neonatal mice, which might result in a higher index value of circulating IgG in the host animals (due to smaller blood and body volumes). Thirdly, no epidermal detachment was observed in human COL17 transgenic (*COL17*$^{m+/+,\,h+}$) mice which had been administered pathogenic BP-IgG. The transgenic mice possessed both human and mouse COL17, and the inflammatory process induced by BP-IgG in this model might be insufficient for blistering or disrupting mouse COL17 dermal-epidermal adhesion. In fact, the BP IgG treated COL17-humanized mice developed the blistering disease because they only express human COL17 and not the murine antigen. Lastly, COL17-humanized mice have a normal mouse immune system in contrast to the study using SCID mice. In this study we have demonstrated a direct induction of human BP lesions in COL17-humanized mice which provides strong and irrefutable evidence that human BP autoantibodies directly cause subepidermal blisters. Humanization of autoantigens in model animals therefore represents a powerful technical approach capable of improving our understanding of this and other autoimmune diseases.

In addition, we have shown that a therapeutic challenge with a recombinant peptide sequence containing the BP pathogenic epitope as a decoy can significantly inhibit the formation of BP skin lesions and decrease disease severity. The epitope(s) for BP autoantibodies are clustered within a limited area of the NC16A domain [10]. This domain resides in the closest portion to the transmembrane domain within the COL17 ectodomain that circulating autoantibodies easily access [16]. Turning this known characteristic of BP antibodies to our advantage, we have been able to design an effective "trap" for the BP autoantibodies by synthesizing a short recombinant peptide harboring the pathogenic BP epitope sequence which is capable of acting as a decoy. Moreover, we have found that, the R1 antigenic peptide, showed a remarkable increased capacity to bind anti-NC16A BP-IgG after

coupling with GST. This is consistent with a previous report in which COL17 NC16A domain peptides were shown to obtain a more beneficial conformation including α-helix and β-turn after linking with GST, in terms of a higher ligand affinity for the substrate by ELISA[17]. Here, we have clearly demonstrated that this epitope decoy strategy has significant potential for the treatment of antibody-mediated autoimmune diseases in clinical practice. Overall, we believe that the novel mouse model we have created and the technical approach we have followed provide a strong basis for future studies that can provide new insight into the pathomechanisms and therapy of human autoimmune diseases.

METHODS

Generation of *COL17* $^{m-/-}$ mouse

A 14.7kb mouse genomic DNA COL17 fragment was cloned from the mouse 129Sv/Ev genomic library (Stratagene, La Jolla, CA). An 11.5 kb *Nhe*I to *Not*I fragment was subcloned to make the targeting vector. The PGK/Neo cassette was inserted between 6bp upstream of the ATG start codon in exon 2 and 1.2kb downstream in intron 2. The targeting vector was transfected by electroporation into 129 Sv/Ev embryonic stem cells, then the correctly targeted ES cell line was microinjected into blastocysts obtained from C57BL/6J mice (Jackson Laboratories; Bar Harbor, ME) to generate chimeric mice, which were then mated with C57BL/6J females. F1 heterozygotes were crossed with C57BL/6J over more than four generations, and then intercrossed to generate *COL17* $^{m-/-}$ mice.

Screening of *COL17* $^{m-/-}$ mice by PCR, RT-PCR, Northern and Western blotting, histology, electron microscopic findings and immunofluorescence study

Please see **Supplementary Methods** online.

Generation of rescued *COL17* $^{m-/-, h+}$ COL17-humanized mice

Transgenic mice (C57BL/6 background) consisting of the squamous epithelial-specific K14 promoter and a human COL17 cDNA (*COL17* $^{m+/+, h+}$) were crossed with heterozygous *COL17* $^{m+/-}$ mice. Animals that carried both the heterozygous null mutation of *COL17* and the transgene of human COL17 (*COL17* $^{m+/-, h+}$) were bred to produce rescued *COL17* $^{m-/-, h+}$ COL17-humanized mice.

Preparation and characterization of IgG fractions from BP patients

Sera were obtained from 5 BP patients during the early, active phase of the disease. IIF was performed using normal human skin as a substrate obtained from surgical operations. The highest dilution of the sera showing positive fluorescence on BMZ was defined as the IIF titer. Autoantibody index values in the patients' sera against COL17 (this index value was referred to the COL17 NC16A domain peptide) and BP230 were measured using ELISA kits as per the manufacturer's instructions (MBL, Japan). The ELISA index value was defined by the following

formula: index= (optical density [OD] of tested serum – OD of negative control) / (OD of positive control – OD of negative control) x 100. The total IgG fractions from these serum samples were prepared by affinity chromatography using HiTrap Protein G HP (Amersham Biosciences, Japan), and a selection (n=3) were followed by affinity purification directed against COL17 NC16A peptide using HiTrap NHS-activated HP column (Amersham) as per the manufacturer's instructions (see Supplementary Method). The IgG fractions were dialyzed against PBS and concentrated by ultrafiltration (Millipore, Lexington, Mass).

Passive transfer studies

Passive transfer of IgG into mice was performed as described previously with minor modifications [4, 5, 9]. Briefly, each mouse received a single intra-peritoneal injection of IgG (dose: 0.05~ 2 mg/g body weight). At 48 hours after the injection, the extent of the skin disease was judged if a distinct Nikolsky sign was observed or not. The animals were then sacrificed and skin samples were studied by light microscopy and direct immunofluorescence microscopy using FITC-conjugated rat anti-human IgG (1:100; Jackson Immunoresearch Laboratories, West Grove, PA).

Generation of recombinant COL17 NC16A peptide

77 amino acids covered with full-length of COL17 NC16A domain (R1, amino acids 490-566), and its 45 amino acids N-terminus half (R2, amino acids 490-534) were both synthesized as GST-fusion proteins using expression vector pGEX2-T (Amersham Biosciences, Japan) and bacteria BL21 (Amersham Biosciences, Japan) as reported previously [1]. In this study, we used both native GST-fusion forms, R1-GST and R2-GST, and GST-cleaved ones (R1, and R2). Other variably sized and distributed amino acids R3 (amino acids 490-525), R4 (amino acids 526-559), R5 (amino acids 490-509), and R6 (amino acids 506-525) peptides were chemically synthesized (R3 and R4; Greiner Bio-one, Japan, R5 and R6; Nippi, Inc, Japan).

Therapeutic study of COL17 NC16A domain antigenic peptide

Preliminarily *in vitro* immune-adsorption studies demonstrated that a 77 amino acid recombinant peptide (R1) most efficiently suppressed the BP antibody index value from BP patient sera (see Fig. 3 b and **Supplementary Method**), we selected to use the R1-GST peptide for the *in vivo* decoy therapy. For the *in vivo* study, each mouse received a subcutaneous injection of 300 μg of R1-GST fusion protein desalted in 20 mM Tris-HCl, pH 7.5 to the dorsal skin soon after and 24 h after a 1 mg intra-peritoneal injection of total IgG from three individual BP patients (n=17). For controls, the same dose of GST was used (n=16).

All mouse procedures were approved by the Institutional Animal Care and Use Committee of Hokkaido University, and fully informed consents from all patients were obtained for the use of their human materials.

Statistical analysis and ethical considerations

Growth differences between groups were examined for statistical significance using analysis of variance (ANOVA) with Fisher's PLSD test. For therapeutic analysis of the effects of synthetic peptide treatments, we determined statistical significance using the Student's *t* test. *P* values less than 0.05 were considered significant.

ACKNOWLEDGEMENTS

We thank Miss Megumi Sato, Ayumi Honda, Akari Nagasaki, and Etsuko Nishizono for their technical assistance. This work was supported in part by Grants-in-Aid for Scientific Research from Japan Society for the Promotion of Science to Shimizu H (15390336, 17209038, 18013002) and Sawamura D (17659331, 18390309, 18659315). Also this was assisted in part by the Project for Realization of Regenerative Medicine from the Ministry of Education, Science, Sports, and Culture of Japan to Shimizu H (2003-2007), and Health and Labour Sciences Research Grants from Ministry of Health and Welfare to Shimizu H (2004-2006), and by NIH grant RO1 AR048982 to Yancey KB.

REFERENCES

1. Jacobson, D.L., Gange, S.J., Rose, N.R., & Graham, N.M.H. Epidemiology and estimated population burden of selected autoimmune diseases in the United States. *Clin Immunol Immunopathol* **84**, 223-243 (1997).
2. Taneja, V. & David, C.S. Lessons from animal models for human autoimmune diseases. *Nat Immunol* **2**, 781-784 (2001).
3. Gregersen, J.W., Holmes, S. & Fugger, L. Humanized animal models for autoimmune diseases. *Tissue Antigens* **63**, 282-394 (2004).
4. Anhalt, G.J., Labib, R.S., Voorhees, J.J., Beals, T.F., & Diaz, L.A. Induction of pemphigus in neonatal mice by passive transfer of IgG from patients with the disease. *N Engl J Med* **306**, 1189-1196 (1982).
5. Roscoe, J.T. *et al.* Brazilian pemphigus foliaceus autoantibodies are pathogenic to BALB/c mice by passive transfer. *J Invest Dermatol* **85**, 538-541 (1985).
6. Madsen, L.S., *et al.* A humanized model for multiple sclerosis using HLA-DR2 and T-cell receptor. *Nat Genet* **23**, 343-347 (1999).
7. Wen, L. *et al.* In vivo evidence for the contribution of human histocompatibility leukocyte antigen (HLA)-DQ molecules to the development of diabetes. *J Exp Med* **191**, 97-104 (2000).